

## Identifying collective modes through impurity pinning in cuprate superconductors

Roy H. Nyberg, Enrico Rossi,<sup>\*</sup> and Dirk K. Morr

*Department of Physics, University of Illinois at Chicago, Chicago, Illinois 60607, USA*

(Received 21 February 2008; published 11 August 2008)

We propose a scanning tunneling spectroscopy experiment to identify the nature and relative strength of collective modes in the high-temperature superconductors (HTSCs). To this end, we show that the pinning of diverse collective modes by impurities leads to qualitatively different fingerprints in the local density of states. These fingerprints directly reflect the modes' magnetic or nonmagnetic character, as well as their wave vectors and correlation lengths. These results provide an alternative method for identifying collective modes not only in the HTSCs but also in other correlated electron systems.

DOI: [10.1103/PhysRevB.78.054504](https://doi.org/10.1103/PhysRevB.78.054504)

PACS number(s): 74.72.-h, 73.20.Mf, 74.25.Ha, 74.25.Jb

Identifying the collective mode that is responsible for the emergence of the superconducting phase and the unconventional normal-state properties of the high-temperature superconductors (HTSCs) is one of the key issues in understanding these complex materials and the focus of an intense scientific debate. The problem in resolving this issue arises from the fact that each proposal for a candidate mode,<sup>1</sup> such as spin or charge modes, or phonons, possesses some experimental support. For example, prominent features in the electronic excitation spectrum of the HTSCs, as observed by angle-resolved photoemission (ARPES) (Refs. 2 and 3) and tunneling<sup>4,5</sup> experiments, were argued to arise from a coupling either to a *magnetic resonance mode*,<sup>2,4</sup> seen in inelastic-neutron-scattering experiments,<sup>6-8</sup> or to phonons.<sup>3,5</sup> The interpretation of these experiments is further complicated by the coupling between various modes.<sup>7,9</sup> Clearly, new experiments are required that can unambiguously identify the collective mode giving rise to the complex behavior of the HTSCs.

In this article, we propose such an experiment based on the idea that different collective modes, when pinned by impurities, exert qualitatively different effects on the local electronic structure of a  $d_{x^2-y^2}$ -wave superconductor. These effects can be measured via scanning tunneling spectroscopy (STS) and hence allow us to directly identify the nature of the pinned mode. In particular, we show that the pinning of spin (charge) modes by impurities induces static spin (charge)-density droplets which act as scattering potentials for the fermionic degrees of freedom and thereby affect the superconductor's local density of states (LDOS). Indeed, static spin droplets around Ni and Zn impurities have been observed in nuclear-magnetic-resonance (NMR) experiments.<sup>10-13</sup> By using the  $\hat{T}$ -matrix<sup>14,15</sup> and Bogoliubov-de Gennes (BdG) (Ref. 16) formalisms, we demonstrate that spin and charge droplets lead to *qualitatively* different fingerprints in the LDOS. For example, in contrast to a pinned charge mode, a pinned (antiferromagnetic) spin mode prevents the creation of resonant impurity states, leads to complementary spatial patterns in the spin-resolved LDOS, and gives rise to a strong magnetic-field dependence of the LDOS. These differences are a direct consequence of the modes' quantum numbers and momentum structures, and thus are robust features that are insensitive to the details of the underlying band structure or of the impuri-

ty's scattering potential. This generality suggests that the same idea can also be used in other correlated electron systems to identify the nature of collective modes.

The coupling of an impurity with spin  $\mathbf{S}_{\text{imp}}$  located at site  $\mathbf{R}$  to collective spin and charge modes, represented by the operators  $\mathbf{s}_e$  and  $n_e$ , respectively, is described by the Hamiltonian<sup>17,18</sup>

$$\mathcal{H}_{\text{int}} = -J\mathbf{S}_{\text{imp}} \cdot \mathbf{s}_e(\mathbf{R}) + U\delta n_e(\mathbf{R}), \quad (1)$$

with  $J, U > 0$  and  $\delta n_e(\mathbf{r}) = n_e(\mathbf{r}) - n_0$ , where  $n_0$  is the uniform charge density. The creation of a static spin droplet requires a nonzero spin polarization of the impurity,<sup>19</sup>  $\langle S_{\text{imp}}^z \rangle$ , which can be induced, for example, by applying a magnetic field  $H \ll H_c^{ab}$  in the  $ab$  plane, thus avoiding complications arising from the creation of an Abrikosov vortex lattice.<sup>21,22</sup> The impurity-mode coupling of Eq. (1) induces static spin-<sup>17</sup> and charge-density oscillations<sup>18</sup> described by

$$\langle s_e^z(\mathbf{r}) \rangle = J \langle S_{\text{imp}}^z \rangle \chi_s(\mathbf{r} - \mathbf{R}, \omega = 0),$$

$$\langle \delta n_e(\mathbf{r}) \rangle = -U \chi_c(\mathbf{r} - \mathbf{R}, \omega = 0), \quad (2)$$

respectively. Here,  $\chi_s(\chi_c)$  is the spin (charge) susceptibility. For the static susceptibilities in momentum space, we make the ansatz  $\chi_{s,c}(\mathbf{q}, \omega = 0) = \chi_0^{s,c} / [\xi_{s,c}^{-2} + (\mathbf{q} - \mathbf{Q}_{s,c})^2]$ , where  $\xi_{s,c}$  is the respective correlation length,  $\mathbf{Q}_s = (\pi, \pi)$ ,<sup>23</sup> and  $\mathbf{Q}_c = 0$ , in agreement with NMR experiments.<sup>10-13,17,24</sup> Note that the results shown below remain valid even for incommensurate modes as long as the wavelength of the incommensuration is larger than  $\xi_{s,c}$ . The mean-field Hamiltonian of the entire system is given by

$$\begin{aligned} \mathcal{H} = & \sum_{\mathbf{r}, \mathbf{r}', \sigma} t_{\mathbf{r}\mathbf{r}'} c_{\mathbf{r}, \sigma}^\dagger c_{\mathbf{r}', \sigma} + \sum_{\mathbf{r}, \mathbf{r}'} [\Delta_{\mathbf{r}, \mathbf{r}'} c_{\mathbf{r}, \uparrow}^\dagger c_{\mathbf{r}', \downarrow}^\dagger + \text{H.c.}] \\ & - \sum_{\mathbf{r}, \alpha, \beta} [g_s \langle s_z(\mathbf{r}) \rangle \sigma_{\alpha\beta}^z + g_c \langle \delta n(\mathbf{r}) \rangle \mathbf{1}_{\alpha\beta}] c_{\mathbf{r}, \alpha}^\dagger c_{\mathbf{r}, \beta}, \quad (3) \end{aligned}$$

where  $c_{\mathbf{r}, \sigma}^\dagger$  creates an electron with spin  $\sigma$  at site  $\mathbf{r}$ ,  $t_{\mathbf{r}\mathbf{r}'}$  is the hopping integral between sites  $\mathbf{r}$  and  $\mathbf{r}'$ , and  $\Delta_{\mathbf{r}, \mathbf{r}'}$  is the  $d_{x^2-y^2}$ -wave superconducting (SC) gap. The last term in Eq. (3) describes the scattering of electrons by the total spin density  $\langle s_z(\mathbf{r}) \rangle = \langle s_e^z(\mathbf{r}) \rangle + \langle S_{\text{imp}}^z \rangle \delta_{\mathbf{r}, \mathbf{R}}$  and effective charge density  $\langle \delta n(\mathbf{r}) \rangle = \langle \delta n_e(\mathbf{r}) \rangle - \delta_{\mathbf{r}, \mathbf{R}}$ . The droplets' scattering strength is determined by only two parameters: for a spin droplet by  $\eta_s = J\chi_s(0, 0)$  and  $\bar{g}_s = g_s \langle S_{\text{imp}}^z \rangle$ , such that

$$g_s \langle s_z(\mathbf{r}) \rangle = \bar{g}_s [\eta_s \chi_s(\mathbf{r} - \mathbf{R}, 0) / \chi_s(0, 0) + \delta_{\mathbf{R}, \mathbf{r}}] \quad (4)$$

and for a charge droplet by  $\eta_c = U \chi_c(0, 0)$  and  $\bar{g}_c = g_c$ .

We study the effects of electronic scattering on the LDOS by using two complementary methods: the  $\hat{T}$ -matrix<sup>14,15</sup> approach, which allows us to investigate large host systems but assumes a spatially constant superconducting order parameter (SCOP), and the BdG (Ref. 16) formalism, which accounts for spatial variations in the SCOP but can treat only small system sizes. Within the  $\hat{T}$ -matrix approach, the Green's-function matrix in Matsubara space is given by<sup>15</sup>

$$\hat{G}(\mathbf{r}, \mathbf{r}', \omega_n) = \hat{G}_0(\mathbf{r}, \mathbf{r}', \omega_n) + \sum_{\mathbf{l}, \mathbf{p}} \hat{G}_0(\mathbf{r}, \mathbf{l}, \omega_n) \hat{T}(\mathbf{l}, \mathbf{p}, \omega_n) \hat{G}_0(\mathbf{p}, \mathbf{r}', \omega_n), \quad (5)$$

where the sum runs over all droplet sites. The  $\hat{T}$  matrix is determined from

$$\hat{T}(\mathbf{l}, \mathbf{p}, \omega_n) = \hat{V}_1 \delta_{\mathbf{l}, \mathbf{p}} + \hat{V}_1 \sum_{\mathbf{s}} \hat{G}_0(\mathbf{l}, \mathbf{s}, \omega_n) \hat{T}(\mathbf{s}, \mathbf{p}, \omega_n), \quad (6)$$

where  $\hat{G}_0 = (i\omega_n \sigma_0 - \varepsilon_{\mathbf{k}} \sigma_3 + \Delta_{\mathbf{k}} \sigma_1)^{-1}$  is the unperturbed Green's function;  $\hat{V}_1 = -g_s \langle s_z(\mathbf{l}) \rangle \sigma^z - g_c \langle \delta n(\mathbf{l}) \rangle \mathbf{1}$ ;

$$\varepsilon_{\mathbf{k}} = -2t(\cos k_x + \cos k_y) - 4t' \cos k_x \cos k_y - \mu \quad (7)$$

is the normal-state tight-binding dispersion, with  $t=300$  meV,  $t'/t=-0.4$ , and  $\mu/t=-1.083$ , representative of the HTSC (Ref. 25); and  $\Delta_{\mathbf{k}} = \Delta_0(\cos k_x - \cos k_y)/2$  is the SC gap, with  $\Delta_0=30$  meV. The LDOS,  $N(\mathbf{r}, \omega) = A_{11}(\mathbf{r}, \omega) - A_{22}(\mathbf{r}, -\omega)$ , with

$$A_{ii}(\mathbf{r}, \omega) = -\frac{1}{\pi} \text{Im} \hat{G}_{ii}(\mathbf{r}, \mathbf{r}, \omega + i\delta) \quad (8)$$

and  $\delta=0.2$  meV, is obtained from Eq. (5). In contrast, in the BdG formalism,<sup>16</sup> one solves the eigenvalue equation

$$\sum_{\mathbf{r}'} \begin{pmatrix} H_{\mathbf{r}\mathbf{r}'}^+ & \Delta_{\mathbf{r}\mathbf{r}'} \\ \Delta_{\mathbf{r}\mathbf{r}'}^* & -H_{\mathbf{r}\mathbf{r}'}^- \end{pmatrix} \begin{pmatrix} u_{\mathbf{r}', n} \\ v_{\mathbf{r}', n} \end{pmatrix} = E_n \begin{pmatrix} u_{\mathbf{r}, n} \\ v_{\mathbf{r}, n} \end{pmatrix}, \quad (9)$$

with  $H_{\mathbf{r}\mathbf{r}'}^{\pm} = t_{\mathbf{r}\mathbf{r}'} + (\mp g_s \langle s_z(\mathbf{r}) \rangle - g_c \langle \delta n(\mathbf{r}) \rangle - \mu) \delta_{\mathbf{r}, \mathbf{r}'}$ , and self-consistently computes the SC gap via

$$\Delta_{\mathbf{r}\mathbf{r}'} = -\frac{V}{2} \sum_n [u_n(\mathbf{r}) v_n(\mathbf{r}') + u_n(\mathbf{r}') v_n(\mathbf{r})] \tanh\left(\frac{E_n}{2k_B T}\right), \quad (10)$$

where the sum runs over all eigenstates of the system.  $V=0.7375t$  yields the same (clean) SC gap as taken in the  $\hat{T}$ -matrix approach. The LDOS is obtained via

$$N(\omega, \mathbf{r}) = \sum_n [u_n^2(\mathbf{r}) \delta(\omega - E_n) + v_n^2(\mathbf{r}) \delta(\omega + E_n)].$$

In order to identify the qualitative effects of spin and charge droplets on the LDOS, we first consider the case when only one of the modes couples to the impurity and present in Fig. 1(a) [Fig. 1(b)] the normalized spin (charge) density for a pure spin (charge) droplet [the center of the

droplet is located at (0,0)].<sup>26</sup> To directly compare the effects of the droplets, we use  $\bar{g}_s = \bar{g}_c$  and  $\xi_c = \xi_s$ , with  $\xi_s = 5a_0$  representative of the underdoped HTSC (Ref. 12) and we present in Figs. 1(c) and 1(d) the LDOS obtained from the  $\hat{T}$ -matrix approach inside the spin and charge droplets, respectively. The low-frequency LDOSs in these two droplets exhibit significant qualitative differences. In the spin droplet, the SC coherence peaks are clearly visible and the LDOS exhibits only weak Friedel-type oscillations but possesses no impurity resonance. In contrast, in the charge droplet, the SC coherence peaks are strongly suppressed and a resonant impurity state exists with corresponding peaks in the LDOS at  $\pm 2$  meV. These qualitatively different effects of the charge and spin droplets on the LDOS arise from the spatial forms of their scattering potentials. For a spin droplet, the alternating sign of  $\langle s_z(\mathbf{r}) \rangle$  and hence of the scattering potential leads to destructive interference of scattered electrons, which prevents the creation of an impurity state inside the SC gap. This interpretation is supported by the fact that the impurity resonance of the decoupled ( $\eta_s=0$ ) impurity [see Fig. 1(e)] shifts to higher energies with increasing  $\eta_s$ , implying a decrease in the effective scattering strength of the impurity. Note also that, while the coherence peaks are absent in the LDOS at the impurity site for a decoupled impurity, the peaks re-emerge in the LDOS with increasing coupling to the collective mode. This leads for sufficiently large  $\eta_s$  to a LDOS that is qualitatively different from that of a decoupled impurity ( $\eta_s=0$ ). In contrast, for the charge droplet, the scattered electrons interfere constructively due to the same sign of the scattering potential at all sites, which leads to an increase in the effective scattering strength. Accordingly, the impurity resonance of the decoupled ( $\eta_c=0$ ) impurity shifts to lower energies with increasing  $\eta_c$  [see Fig. 1(f)]. The modes' different momentum dependence thus leads to distinct signatures of a spin [Fig. 1(c)] and a charge [Fig. 1(d)] droplet in the LDOS. Finally, note that the pinning of phonons by impurities, as well as the resulting static lattice distortions, should give rise to a nonmagnetic scattering term in Eq. (1) that is similar to that of a charge droplet. Consequently, we expect the qualitative effects of pinned phonons and charge modes on the LDOS to be quite similar.

An important fingerprint of the spin droplet can be found in the spatial structure of the spin-resolved LDOS, as shown in Figs. 2(a) and 2(b), where we present the spin- $\uparrow$  and spin- $\downarrow$  LDOSs at adjacent sites. As expected from the spatially alternating sign of the scattering potential, the frequency dependence of the spin- $\uparrow$  LDOS at  $\mathbf{r}=(1, 0)$  is qualitatively similar to that of the spin- $\downarrow$  LDOS at  $\mathbf{r}=(2, 0)$ , and vice versa. This behavior is observed for all sites of the droplet that belong to different (antiferromagnetic) sublattices. As a result, the spin- $\uparrow$  and spin- $\downarrow$  LDOSs possess spatially complementary intensity patterns, as shown in Figs. 2(c) and 2(d), with the spin- $\uparrow$  LDOS being large at those sites where the spin- $\downarrow$  LDOS is small and vice versa. In contrast, in a charge droplet, the spin- $\uparrow$  and spin- $\downarrow$  LDOSs are identical. This qualitative difference is directly linked to the modes' quantum numbers, which determine their coupling to the electrons.

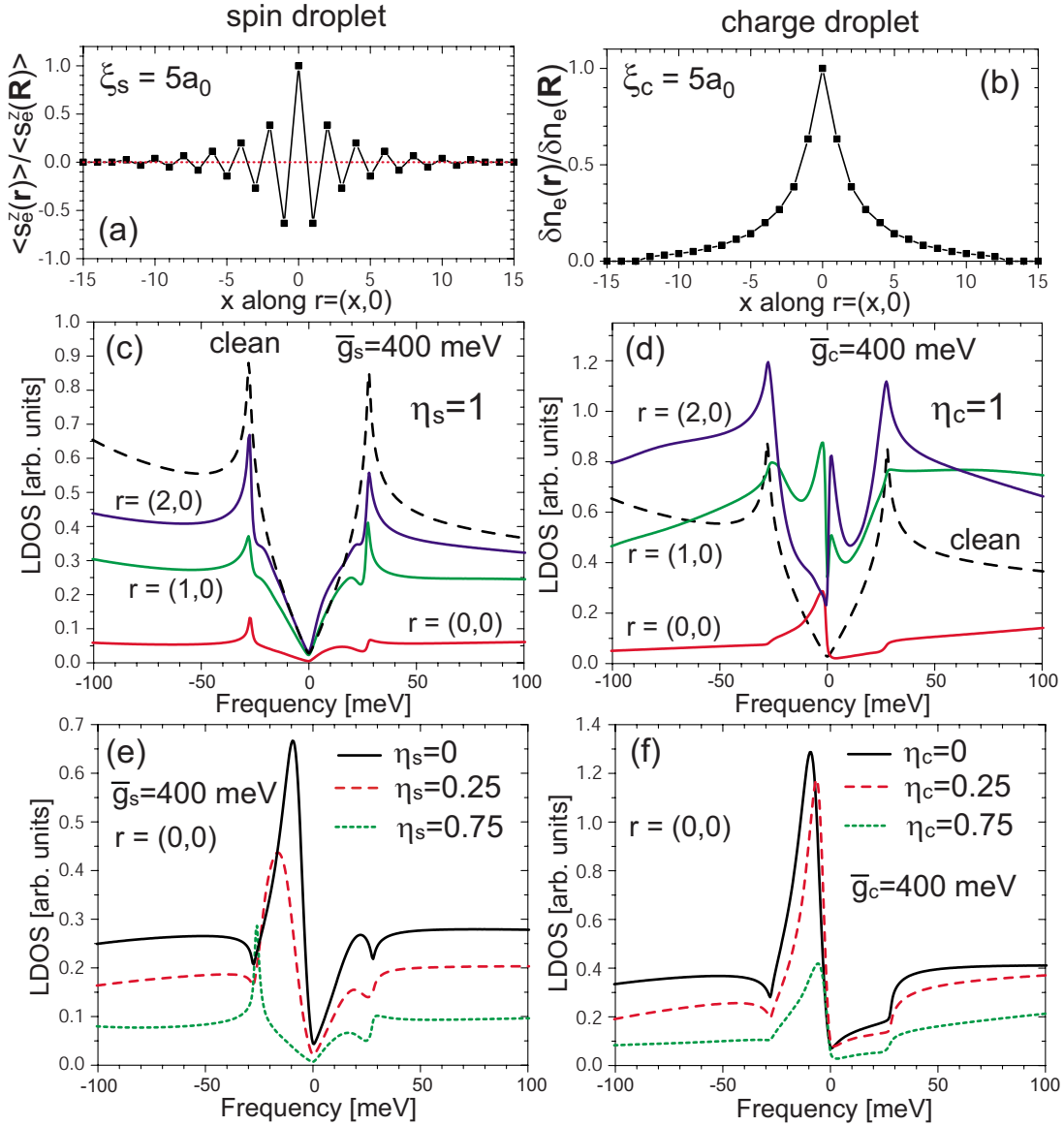


FIG. 1. (Color online) Normalized (a) spin and (b) charge densities along  $\mathbf{r}=(x,0)$ . LDOS inside (c) a spin and (d) a charge droplet with  $\eta_{s,c}=1$  and  $\bar{g}_s, \bar{g}_c=400$  meV (the dashed lines represent the clean LDOS). Evolution of the LDOS with increasing  $\eta_{s,c}$  for (e) a spin and (f) a charge droplet.

Another qualitative difference between spin and charge droplets arises from the magnetic-field dependence of the impurity's spin polarization  $\langle S_{\text{imp}}^z(H, T) \rangle = CH/(T + \Theta)$ .<sup>13</sup> Since  $\bar{g}_s = g_s \langle S_{\text{imp}}^z(H, T) \rangle$ , it immediately follows that the droplet's scattering strength and hence the resulting LDOS are expected to change with  $H$  and  $T$ . To demonstrate this effect, we present in Fig. 3(a) the total LDOSs for several values of  $\bar{g}_s$  representing different magnetic fields. Consider, for example, that a given  $H_0 \ll H_{c2}^{ab}$  corresponds to  $\bar{g}_s = 100$  meV. Increasing the magnetic field to  $2H_0$  ( $\bar{g}_s = 200$  meV) or  $4H_0$  ( $\bar{g}_s = 400$  meV) leads to a suppression of the LDOS in the droplet.<sup>27</sup> Since the coupling between impurity and a charge mode is unaffected by the magnetic field, the observation of a magnetic-field-dependent LDOS as shown in Fig. 3(a) is an important signature of a static spin droplet.

In general, an impurity possesses both a magnetic and a

nonmagnetic scattering potential. However, as long as only one type of collective mode is present, the resulting LDOS is quantitatively very similar to that shown in Fig. 1. In contrast, if both charge and spin modes exist in the superconductor and simultaneously couple to the impurity, we find that the properties of the resulting LDOS are determined by the ratio  $\alpha = \bar{g}_c \eta_c / \bar{g}_s \eta_s$ , as shown in Fig. 3(b) for  $\alpha = 1/3$ . As  $\alpha$  changes from 0 to  $\infty$ , the LDOS changes continuously from being “spinlike” [Fig. 1(c)] to being “chargelike” [Fig. 1(d)]. However, even in this more complicated situation, the modes' relative strength can be extracted from the  $H$  dependence and spatial form of the spin-resolved LDOS.

The pair-breaking nature of impurities in  $d_{x^2-y^2}$ -wave superconductors leads to the suppression of the SCOP, an effect that is not taken into account in the  $\hat{T}$ -matrix approach. To study the relevance of this suppression, we compare the results of the  $\hat{T}$ -matrix approach with those of the BdG formal-

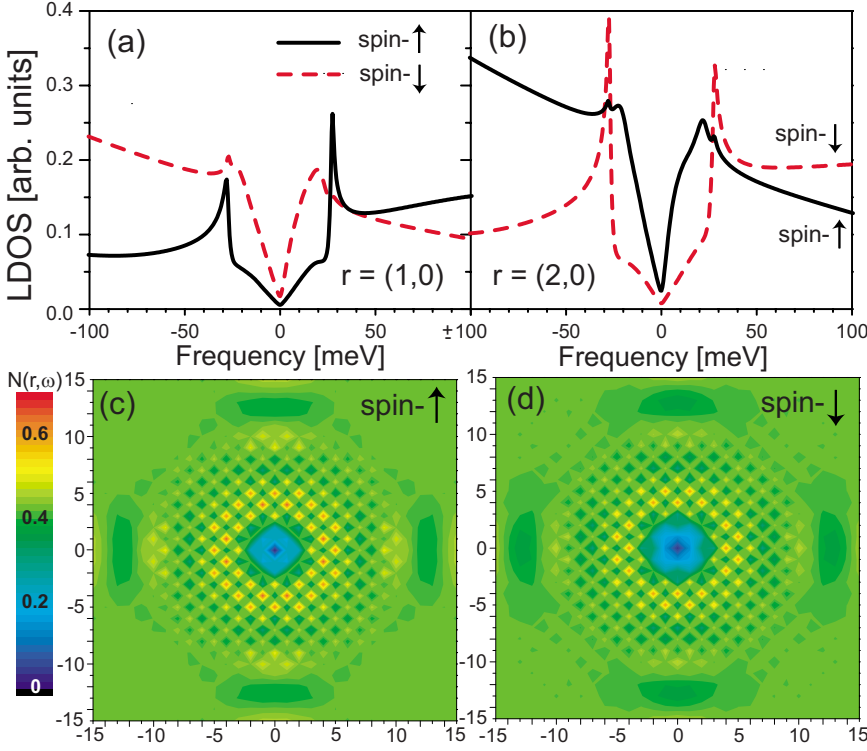


FIG. 2. (Color online) Spin-resolved LDOS for  $\bar{g}_s=400$  meV at adjacent sites (a)  $\mathbf{r}=(1,0)$  and (b)  $\mathbf{r}=(2,0)$ . Intensity plot of the (c) spin- $\uparrow$  and (d) spin- $\downarrow$  LDOSs at the frequency of the holelike coherence peak,  $\omega_{cp}=30$  meV.

ism. In Fig. 4(a) we present the spatial form of the SCOP [see Eq. (10)] in a spin droplet for a system with  $N=60 \times 60$  sites and the same parameters as above. The SCOP is significantly suppressed only near the center of the droplet and quickly recovers its bulk value within a few lattice spacings from the center. To ascertain how the SCOP's suppression affects the LDOS, we compare in Fig. 4(b) [Fig. 4(c)] the results of the  $\hat{T}$ -matrix and BdG approaches for the spin- $\downarrow$  (spin- $\uparrow$ ) LDOSs at  $\omega_{cp}=30$  meV. Both LDOS are in good qualitative agreement and exhibits the same oscillations characteristic of the antiferromagnetic nature of the droplet. The quantitative differences are minimal: first, the LDOS of the BdG approach undergoes a  $\pi$ -phase shift at  $\Delta r \approx 10a_0$  from the center of the droplet, which is absent for the  $\hat{T}$ -matrix results. Second, at  $\mathbf{r}=(0,0)$ , the spin- $\uparrow$  LDOS of the two approaches is out of phase. A detailed analysis shows

that this effect arises from a decrease in the droplet's effective scattering strength due to the suppression of the SCOP. Since similar good agreement is obtained for a charge droplet, we conclude that the suppression of the SCOP has only minor quantitative effects on the LDOS.

While we considered above a static spin droplet, we recently also studied the effects of a single fluctuating magnetic impurity (for zero magnetic field) on the STS spectra.<sup>28</sup> We found characteristic signatures of the fluctuating impurity in the STS spectra as long as the impurity's fluctuation time satisfies  $\tau_s \gg 1/E_F$ . This suggests that the results shown above for  $H \neq 0$  might remain valid even for  $H=0$  as long as the fluctuation time of the spin droplet (created from the coupling of the mode to a fluctuating magnetic impurity) is sufficiently long. This fluctuation time increases with increasing damping of the spin excitations and becomes infinite when the damping exceeds a critical value,<sup>29</sup> in which

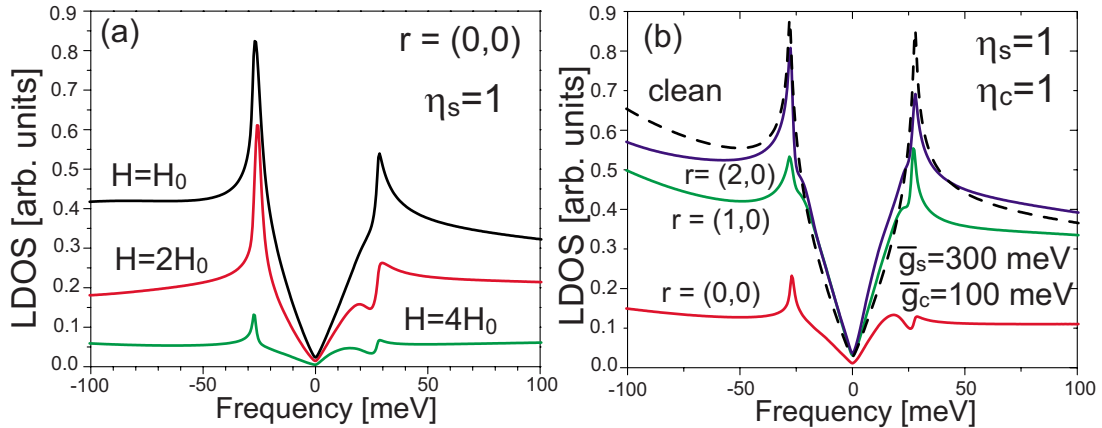


FIG. 3. (Color online) (a) Total LDOS for a spin droplet at  $\mathbf{r}=(0,0)$  for several  $\bar{g}_s=g_s \langle S_{imp}^z(H, T) \rangle (U=0)$ . (b) Total LDOS for a droplet with  $\langle s_z(\mathbf{r}) \rangle, \langle \delta n(\mathbf{r}) \rangle \neq 0$  and  $\alpha=1/3$ .

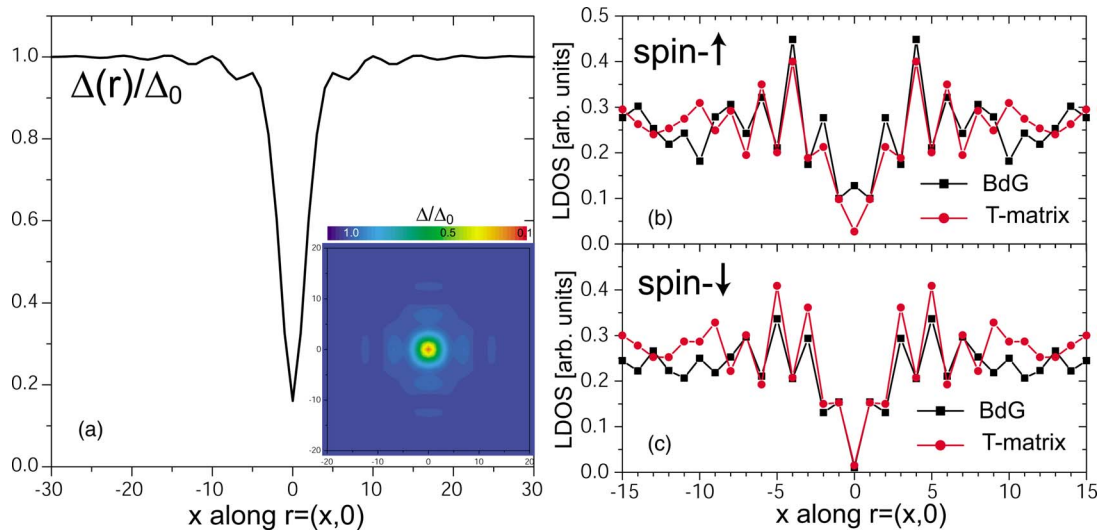


FIG. 4. (Color online) (a) SCOP along  $\mathbf{r}=(x,0)$  for a spin droplet. Inset: intensity plot of the SCOP. (b) Spin- $\uparrow$  and (c) spin- $\downarrow$  LDOSs of the  $\hat{T}$ -matrix (red line) and BdG (black line) approaches at  $\omega_{cp}=30$  meV along  $\mathbf{r}=(x,0)$ .

case the droplet becomes static. As a result, it might be possible to find signatures of static (or quasistatic) spin droplets in the LDOS even in the absence of a magnetic field. Note that the effects of dynamic collective modes on quasiparticle interference patterns in the LDOS were discussed in Refs. 18 and 30.

Finally, we note that the STS experiments performed to date in the vicinity of impurities<sup>31–33</sup> were performed in the absence of a magnetic field and have not provided any direct evidence for the presence of a static spin- or charge-density wave. As such, these experiments cannot be directly compared to the results shown above. However, the sharp coherence peaks seen by Hudson *et al.*<sup>33</sup> in the LDOS at the site of a magnetic Ni impurity might represent, as discussed above, a signature of a static (or quasistatic) spin-density wave.

In conclusion, we have shown that the pinning of collective spin or charge modes leads to qualitatively different sig-

natures in the LDOS of a  $d_{x^2-y^2}$  superconductor. In particular, a spin droplet suppresses resonant impurity states, leads to complementary spatial patterns in the spin-resolved LDOS, and gives rise to a strong magnetic-field dependence of the LDOS. In contrast, a charge droplet induces a low-energy impurity resonance and shows no magnetic-field dependence. The generality of these results show that impurities can be used to identify the nature of collective modes not only in the HTSCs but also in other correlated electron systems.

We would like to thank J. C. Davis and D. Maslov for helpful discussions and the Aspen Center for Physics for its hospitality. D.K.M. acknowledges financial support by the Alexander von Humboldt Foundation, the NSF under Grant No. DMR-0513415, and the U.S. DOE under Grant No. DE-FG02-05ER46225.

\*Present address: Condensed Matter Theory Center, Department of Physics, University of Maryland, College Park, MD 20742-4111, USA.

<sup>1</sup>C. Castellani, C. Di Castro, and M. Grilli, *Z. Phys. B: Condens. Matter* **103**, 137 (1997); A. Abanov, A. V. Chubukov, and J. Schmalian, *Adv. Phys.* **52**, 119 (2003); S. A. Kivelson, I. P. Bindloss, E. Fradkin, V. Oganesyan, J. M. Tranquada, A. Kapitulnik, and C. Howald, *Rev. Mod. Phys.* **75**, 1201 (2003); M. Eschrig, *Adv. Phys.* **55**, 47 (2006).

<sup>2</sup>J. C. Campuzano, H. Ding, M. R. Norman, H. M. Fretwell, M. Randeria, A. Kaminski, J. Mesot, T. Takeuchi, T. Sato, T. Yokoya, T. Takahashi, T. Mochiku, K. Kadowaki, P. Guptasarma, D. G. Hinks, Z. Konstantinovic, Z. Z. Li, and H. Raffy, *Phys. Rev. Lett.* **83**, 3709 (1999).

<sup>3</sup>G.-H. Gweon, T. Sasagawa, S. Y. Zhou, J. Graf, H. Takagi, D. H. Lee, and A. Lanzara, *Nature (London)* **430**, 187 (2004).

<sup>4</sup>J. F. Zasadzinski, L. Ozyuzer, N. Miyakawa, K. E. Gray, D. G. Hinks, and C. Kendziora, *Phys. Rev. Lett.* **87**, 067005 (2001).

<sup>5</sup>J. Lee, K. Fujita, K. McElroy, J. A. Slezak, M. Wang, Y. Aiura, H. Bando, M. Ishikado, T. Masui, T. J. -X. Zhu, A. V. Balatsky, H. Eisaki, S. Uchida, and J. C. Davis, *Nature (London)* **442**, 546 (2006).

<sup>6</sup>J. Rossat-Mignod, L. P. Regnault, C. Vettier, P. Bourges, P. Bulet, J. Bossy, J. Y. Henry, and G. Lapertot, *Physica C* **185-189**, 86 (1991); H. A. Mook, M. Yethiraj, G. Aeppli, T. E. Mason, and T. Armstrong, *Phys. Rev. Lett.* **70**, 3490 (1993); P. Bourges, L. P. Regnault, Y. Sidis, and C. Vettier, *Phys. Rev. B* **53**, 876 (1996); P. Dai, M. Yethiraj, H. A. Mook, T. B. Lindemer, and F. Dogan, *Phys. Rev. Lett.* **77**, 5425 (1996); H. F. Fong, P. Bourges, Y. Sidis, L. P. Regnault, A. Ivanov, G. D. Gu, N. Koshizuka, and B. Keimer, *Nature (London)* **398**, 588 (1999); C. Stock, W. J. L. Buyers, R. Liang, D. Peets, Z. Tun, D. Bonn, W.

- N. Hardy, and R. J. Birgeneau, Phys. Rev. B **69**, 014502 (2004).
- <sup>7</sup>J. M. Tranquada, in *Handbook of High-Temperature Superconductivity Theory and Experiment*, edited by Robert J. Schrieffer (Springer, New York, 2007), Chap. XXXII.
- <sup>8</sup>S. Pailhes, P. Bourges, Y. Sidis, C. Bernhard, B. Keimer, C. T. Lin, and J. L. Tallon, Phys. Rev. B **71**, 220507(R) (2005).
- <sup>9</sup>D. Reznik, L. Pintschovius, M. Ito, S. Iikubo, M. Sato, H. Goka, M. Fujita, K. Yamada, G. D. Gu, and J. M. Tranquada, Nature (London) **440**, 1170 (2006).
- <sup>10</sup>J. Bobroff, H. Alloul, Y. Yoshinari, A. Keren, P. Mendels, N. Blanchard, G. Collin, and J. F. Marucco, Phys. Rev. Lett. **79**, 2117 (1997).
- <sup>11</sup>M. H. Julien, T. Feher, M. Horvatic, C. Berthier, O. N. Bakharev, P. Segransan, G. Collin, and J. F. Marucco, Phys. Rev. Lett. **84**, 3422 (2000).
- <sup>12</sup>S. Ouazi, J. Bobroff, H. Alloul, and W. A. MacFarlane, Phys. Rev. B **70**, 104515 (2004).
- <sup>13</sup>S. Ouazi, J. Bobroff, H. Alloul, M. Le Tacon, N. Blanchard, G. Collin, M. H. Julien, M. Horvatic, and C. Berthier, Phys. Rev. Lett. **96**, 127005 (2006).
- <sup>14</sup>Y. Lu, Acta Phys. Sin. **21**, 75 (1965); H. Shiba, Prog. Theor. Phys. **40**, 435 (1968).
- <sup>15</sup>N. A. Stavropoulos and D. K. Morr, Phys. Rev. B **73**, 140502(R) (2006).
- <sup>16</sup>P. G. de Gennes, *Superconductivity of Metals and Alloys* (Addison-Wesley, New York, 1989).
- <sup>17</sup>D. K. Morr, J. Schmalian, R. Stern, and C. P. Slichter, Phys. Rev. B **58**, 11193 (1998).
- <sup>18</sup>D. Podolsky, E. Demler, K. Damle, and B. I. Halperin, Phys. Rev. B **67**, 094514 (2003); L. Dell'Anna, J. Lorenzana, M. Capone, C. Castellani, and M. Grilli, *ibid.* **71**, 064518 (2005).
- <sup>19</sup>Previous studies of single impurities (Ref. 20) considered  $S_{\text{imp}} \rightarrow \infty$  and thus found  $\langle S_{\text{imp}}^z \rangle \neq 0$  even for  $H=0$ .
- <sup>20</sup>A. V. Balatsky, I. Vekhter, and J. X. Zhu, Rev. Mod. Phys. **78**, 373 (2006).
- <sup>21</sup>Since  $H_{c2}^{ab} \gg H_{c2}^c$ , the effects of screening currents can be neglected for reasonable in-plane fields.
- <sup>22</sup>K. A. Moler, J. R. Kirtley, D. G. Hinks, T. W. Li, and M. Xu, Science **279**, 1193 (1998).
- <sup>23</sup>D. J. Scalapino, Phys. Rep. **250**, 329 (1995); D. K. Morr and D. Pines, Phys. Rev. Lett. **81**, 1086 (1998).
- <sup>24</sup>J. W. Harter, B. Andersen, J. Bobroff, M. Gabay, and P. Hirschfeld, Phys. Rev. B **75**, 054520 (2007).
- <sup>25</sup>A. Damascelli, Z. Hussain, and Z.-X. Shen, Rev. Mod. Phys. **75**, 473 (2003).
- <sup>26</sup>Due to computational limitations, we set  $\langle s_e^z(\mathbf{r}) \rangle$ ,  $\langle \delta n_e(\mathbf{r}) \rangle = 0$  for  $|\mathbf{r}-\mathbf{R}| > 2\xi_{s,c}$ . This leads to only minor quantitative changes due to the exponential decay of the droplet's amplitude.
- <sup>27</sup>Note that for a decoupled impurity ( $\eta_s=0$ ), the impurity resonance shifts to lower frequencies with increasing  $H$ .
- <sup>28</sup>D. K. Morr and R. H. Nyberg, Phys. Rev. B **68**, 060505(R) (2003).
- <sup>29</sup>A. J. Millis, D. K. Morr, and J. Schmalian, Phys. Rev. Lett. **87**, 167202 (2001).
- <sup>30</sup>A. Polkovnikov, M. Vojta, and S. Sachdev, Phys. Rev. B **65**, 220509(R) (2002); J. H. Han, *ibid.* **67**, 094506 (2003); C. T. Chen and N. C. Yeh, *ibid.* **68**, 220505(R) (2003); J. X. Zhu, Jun Sun, Qimiao Si, and A. V. Balatsky, Phys. Rev. Lett. **92**, 017002 (2004).
- <sup>31</sup>A. Yazdani, C. M. Howald, C. P. Lutz, A. Kapitulnik, and D. M. Eigler, Phys. Rev. Lett. **83**, 176 (1999).
- <sup>32</sup>S. H. Pan, E. W. Hudson, K. M. Lang, H. Eisaki, S. Uchida, and J. C. Davis, Nature (London) **403**, 746 (2000).
- <sup>33</sup>E. W. Hudson, K. M. Lang, V. Madhavan, S. H. Pan, H. Eisaki, S. Uchida, and J. C. Davis, Nature (London) **411**, 920 (2001).